Modelling the Influence of Differential Aeration in Underground Corrosion

R.M. Azoor[1], R.N. Deo[1], N. Birbilis[2], J.K. Kodikara[1]

[1]Department of Civil Engineering, Monash University, Clayton, VIC3800, Australia
[2]Department of Materials Science and Engineering, Monash University, Clayton, VIC3800, Australia

Abstract: Corrosion of buried infrastructure, such as pipelines, is an issue that leads to significant economic loss. Corrosion induced pipe failures are increasingly encountered by water utilities with aging pipe networks around the world. Macro corrosion cells formed due to differential aeration in soil are known to cause significant levels of localised patch corrosion, which can lead to the loss of structural integrity of buried pipelines. This paper presents a finite element model developed using COMSOL Multiphysics® software to identify and characterise regions experiencing high levels of underground corrosion due to differential aeration. Electrochemical reactions on the pipe surface are coupled with the reactant transport mechanisms - through the soil to the pipe depth. Closed form equations are used to characterise the electrical and mass transport properties of the three-phase soil medium using common soil parameters that include porosity and the degree of saturation. The present model enables a study of the effects of variations in soil properties and external conditions on pipeline corrosion. Model results agree well with results presented in the literature and case studies conducted at pipe failure sites in the field. It is envisaged that the model developed herein will enable the water utilities to develop predictive tools that may be useful in condition assessment.

Key words: underground corrosion, differential aeration, finite element modelling

1 Introduction

In a practical sense, it is difficult to locate and predict regions of buried pipeline undergoing corrosion, due to lack of access to the underground asset, and usually, a lack of information related to the asset condition. Furthermore, it is challenging to develop empirically based predictive lifetime equations owing to the difficulty in collecting sufficient data over an asset lifetime that are both accurate and span the range of relevant variables. To circumvent these problems, empirical and statistical methods have been previously used to characterise underground corrosion[1],[3],[4]. However the accuracy of these methods also relies on actual data and field observations. These challenges have necessitated a method to locate and predict the condition of a buried pipeline without physical exhumation and examination. With an understanding of soil as an electrolyte and the mechanisms involved, the electrochemical theory can be used to characterize corrosion in soils[4]. Past research and field evidence show that the level of aeration of soils, and in particular the differences in aeration, plays a significant role in the rates of underground corrosion[1],[4],[5]. The soil properties controlling aeration including porosity and saturation control secondary properties such as resistivity which, when used as the sole indicator for underground corrosion has shown limited success[3], [6]. Therefore a model taking into account the direct and consequential results of soil aeration may solve the problems encountered in soil corrosion. This paper presents a finite element model developed using COMSOL Multiphysics® to characterize underground corrosion influenced by differential aeration and its long term effects. This model couples together mechanisms of diffusion control, active area and corrosion product dynamics to demonstrate the detrimental long term effects of underground corrosion due to differential aeration.

2 Differential Aeration and underground corrosion

The spatial separation of regions on a metal surface with different surface potentials results in the formation of macro corrosion couples. Macro couples could arise from variations of several soil properties from which differential aeration takes a significant role[1],[4],[6]. The formation of insoluble corrosion products creates a shielding effect[4], [8] and also passivates the metal thermodynamically[9], selectively restricting the anodic reaction eventually leading to macro cell formation. This means that spatial variations in soil properties controlling aeration including porosity and degree of saturation can result in the formation of corrosion cells. In

addition to the soil properties, external features that promote or inhibit soil aeration could also result in the formation of differential aeration cells. Impermeable covers such as surface paving, driveways and the presence of vegetation and root zones can be cited as examples. Once formed, the rate of corrosion in a differential aeration couple could be significantly increased by a high ratio of cathode to anode surface area as it increases the corrosion current of the cell[1], [5]. Over long periods of time such localization of the corrosion reaction lead to corrosion patch formation and it has been shown that these corrosion patches are responsible for most pipe failures[10], [11].

3 COMSOL Multiphysics® Simulation

3.1 Model development

A 3D model geometry was created to simulate a section of pipe running through a block of soil with an impermeable cover over half of the ground surface exposed to the atmosphere. This is achieved by imposing a constant concentration boundary condition on one half of the top surface of the block. This illustrates a situation similar to a pipe running through a driveway which restricts the diffusion of oxygen to the pipe lying in the covered region thus promoting the formation of a differential aeration cell. The soil block has dimensions 10x3x3 m and the pipe is of diameter 0.3m lies at a depth of 1m below the surface. Physics dependent meshing was chosen with a finer element size close to the pipe surface.

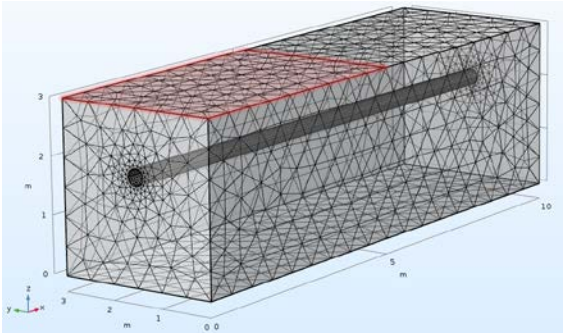

Figure 1: Model geometry showing covered region (depicted by the red shading) and pipe running through

Iron being the major constituent of pipeline alloys including cast iron, ductile iron and steel, the anodic reaction is considered to be the oxidation of iron.

$$Fe \rightarrow Fe^2 + 2\,e^- \quad (1)$$

Most soils having neutral to basic conditions, the cathodic reaction was considered to be the reduction of oxygen[4].

$$O_2 + 2\,H_2O + 4\,e^- \rightarrow 4\,(OH)^- \quad (2)$$

For underground corrosion, the anodic reaction is under activation control and the cathodic reaction is under concentration control[4]. Hence the corresponding current densities for the above two reactions are expressed using Tafel laws as,

$$i_{Fe} = i_{0_{Fe}} \times 10^{\frac{\eta_{Fe}}{A_{Fe}}} \quad (3)$$

for the anodic reaction and,

$$i_{O2} = \frac{C_{O2}}{C\_O2\_ref} \times i_{0_{O2}} \times 10^{\frac{\eta_{O2}}{A_{O2}}} \quad (4)$$

for the cathodic reaction, where $i_{0_{Fe}}$ and $i_{0_{O2}}$ are the respective exchange current densities. The concentration polarization effect is included in the cathodic current density expression as described by Kranc and Sagues[12] where C_{O2} is the concentration of the diffusing oxygen and C_O2_ref is the reference oxygen concentration (atmospheric). A_{Fe} and A_{O2} are the Tafel slopes and η_{Fe} and η_{O2} are the respective over-potentials given by,

$$\eta_{Fe} = -\phi_l - E_{eqFe} \quad (5)$$

and

$$\eta_{O2} = -\phi_l - E_{eqO2} \quad (6)$$

where, is the electrolyte potential of the soil medium and E_{eqO2} and E_{eqFe} are the equilibrium potentials for the cathodic and anodic reactions respectively. The Tafel slopes and the other polarization parameters were sourced from literature. The above equations were included as boundary conditions in the secondary current distribution physics interface in COMSOL Multiphysics®.

3.2 The soil electrolyte

Soil is a heterogeneous medium with three different phases-solid, liquid and gas with the solids forming a capillary-porous structure and the liquid and gas occupying the pore network. The soil properties such as porosity, degree of saturation, level of compaction will change the properties of this three-phase electrolyte and will reflect in the level of corrosivity of the soil. Soil resistivity or conductivity is used to characterize the soil as an electrolyte which is also the chosen parameter associated with soil corrosion in many studies[3], [13]–[17]. To characterize soil as an electrolyte in the model, The closed form equation developed by Mualem & Friedman[18] which builds upon previous work by Rhoades et al.[19] was used for this work. The equation for the bulk soil solution EC_b defined as,

$$EC_b = EC_w.\frac{\theta^{n+2}}{\theta_{sat}} \quad (7)$$

where, EC_b is the electrical conductivity of the bulk soil solution, EC_w, the conductivity of the pore water and n, the porosity. θ and θ_{sat} are the volumetric water content of the soil and the saturated volumetric

content, corrected for bound water so that, $\theta = \Theta - \Theta_0$. The volumetric water contents in this equation were written in terms of the soil porosity (n) and the degree of saturation (S_r) as follows and was input into COMSOL® as an analytic function.

$$EC_b = EC_w \cdot \frac{(n.S_r - \Theta_0)^{n+2}}{n - \Theta_0} \quad (8)$$

The function is called to define the electrolyte conductivity based on soil properties and is used in running parametric sweeps for different situations.

3.3 Oxygen diffusion and cathodic control

In most natural soils metal corrosion proceeds chiefly through cathodic control, as a result of the limiting oxygen transport to the metal surface[4]. Under isobaric and isothermal conditions, the dominant mode of transport of oxygen in soil is diffusion[4]. Diffusion is modelled using Fick's laws with an effective diffusion coefficient adjusted for tortuosity factors and the reduction in cross sectional area available for diffusion due to the porosity and moisture content of soil. The Millington & Quirk model[20] for unsaturated soils, although widely accepted, considers diffusion only through the air filled pores, and neglects the water phase diffusion. Although very small when compared to the diffusion in the air phase, the diffusion of oxygen through water also could contribute to the corrosion process. Aachib et al. [21] proposed the following model including the diffusion through both phases.

$$D_e = \frac{1}{\phi^2}[D_a^0 \theta_{0,a}^p + H D_w^0 \theta_{0,w}^p] \quad (9)$$

where, D_e is the effective diffusion coefficient in both phases, D_a^0, the diffusion coefficient of oxygen in free air, D_w^0, that of free water $\theta_{0,a}$ and $\theta_{0,w}$ are volumetric air and water contents respectively and H is Henry's equilibrium constant and p is a calculated or approximated exponent. As in the previous case the volumetric water and air contents were written in terms of n and S_r to give the following equation.

$$D_e = \frac{1}{n^2} \cdot [D_a^0 \big(n(1 - S_r)\big)^p + H D_w^0 (n S_r)^p] \quad (10)$$

This equation too was used as an analytic function to be called to define the soil property dependent oxygen transport properties.

3.4 Active area of corrosion

The interface of the soil and the corroding metal is heterogeneous and the corrosion reaction occurs only at the areas in contact with the electrolyte. This is termed the active area and has been shown to be directly proportional to the bulk soil conductivity[22], [23]. The reason for this is that, the anodic reaction of iron dissolution needs an aqueous medium and therefore occurs at the regions of electrolyte contact. Lower degrees of saturation would lead to low active areas and full saturation would lead to the highest active area, being the same as the original area of the surface. Therefore, the corrosion rates that are measured in electrochemical experiments need to be corrected based on the active area. Dang et al.[22] showed using electrochemical impedance spectroscopy (EIS) that the electrical conductivity is proportional to the active area and used it to correct the measured corrosion rates. Without active area being considered, the computed corrosion current density is assumed to be distributed over the entire surface of the electrode. This is an over estimation of the experimentally measured current density. Thus, to model the current density obtained experimentally, the true current density needs to be adjusted for active area using conductivity ratios. This modification as described by Dang et al.[22] was included in the anodic current density term.

4 Corrosion products and time-dependent behaviour

The current densities are related to the change in mass of charged species according to Faraday's law of electrolysis. Hence, the molar flux of iron lost by corrosion is given by,

$$N_{Fe} = \frac{-\upsilon_{Fe} . i_{Fe}}{n_{Fe} F} \quad (11)$$

And the molar flux of $(OH)^-$ is given by

$$N_{OH-} = \frac{-\upsilon_{OH-} . i_{OH-}}{n_{OH-} F} \quad (12)$$

where F is Faraday's constant and n_{Fe} and n_{OH-} are the number of electrons involved in the respective redox reactions. $-\upsilon_{Fe}$ and $-\upsilon_{OH-}$ are the stoichiometric coefficients for respective reactions. The above fluxes can be converted to a thickness given the density and molar mass of the species involved. Thus the loss of iron due to corrosion is modelled as a decrease in thickness while the corrosion product deposition is modelled as an increasing thickness of the electrode. The corrosion product was considered to be Iron III Hydroxide ($Fe(OH)_3$) or hydrated iron oxide ($Fe_2O_3.H_2O$) which is commonly identified as a reddish brown deposit in corroding iron[4], [9], [24]. This product is formed by the following reactions

$$Fe^{2+} + 2\,(OH)^- \rightleftharpoons Fe(OH)_2 \quad (13)$$

$$Fe(OH)_2 + (OH)^- \rightleftharpoons Fe(OH)_3 + e^- \quad (14)$$

The loss of metal was calculated based on the current density of the anodic reaction (equation 1) while the corrosion product deposition was calculated from the $(OH)^-$ current density the cathodic reaction (equation 2). The stoichiometric coefficient (υ_{OH-}) for the

cathodic reaction molar flux was taken to be that of $Fe(OH)_3$ formation from the above reactions (equations 13 and 14). Hence the rate of thickness gain or loss of products in meters per second is,

$$V_{Fe} = \frac{N_{Fe}\, m_{Fe}}{\rho_{Fe}} \quad (15)$$

$$V_{FeOH3} = \frac{N_{OH}\, m_{FeOH3}}{\rho_{FeOH3}} \quad (16)$$

where m_{Fe}, ρ_{Fe} and m_{FeOH3}, ρ_{FeOH3} are the molar mass and density of the iron and iron III hydroxide respectively. Passivation of the metal surface was modelled as a result of the shielding effect of corrosion products in a similar approach to that taken by Chang et al [24]. Chang et al used the surface coverage of iron hydroxide corrosion products to weight the contributions of active and passive current densities. In the present work, the effect of passivation was included by a sigmoid function modifying the anodic current density depending on the thickness of the corrosion product layer formed. As a rough approximation, the hinge point of this sigmoid function was chosen to be 1mm, thus diminishing the corrosion rate for corrosion products in a macro scale. The thickness of the Iron III hydroxide layer formed is a time dependent quantity calculated by integrating the rate of growth of $Fe(OH)_3$ over time.

With the above relations given as inputs, the soil medium is characterized using the degree of saturation and the porosity, and the time dependent with initialization solution method in COMSOL was used to calculate the electric potential distribution, oxygen concentration and the resulting anodic and cathodic current densities on the pipe surface. A total time period of 5000 days (≈14 years) was simulated, allowing enough time for long term trends of corrosion to develop. A parametric sweep was performed for the degree of saturation S_r, varying it from 0.1 to 0.9 with a 0.1 increment.

5 Results and Discussion

Time dependent trends of electrolyte potential and current, and the electrode potential showed the formation of a macro corrosion cell due to the effect of differential aeration. The results are compared in the region covered by the impermeable barrier, and the region which is open to the atmosphere, hereafter referred to as closed and open regions respectively. The low access to oxygen in the closed region leads to a higher electrolyte potential in that region and the formation of corrosion products rapidly on the pipe in the open region diminishes the corrosion current. The corrosion current in the open region then becomes larger than that of the open region forming a "corrosion hotspot" in the covered region. A net electrolyte current then flows through the soil electrolyte from the anodic closed region to the cathodic open region.

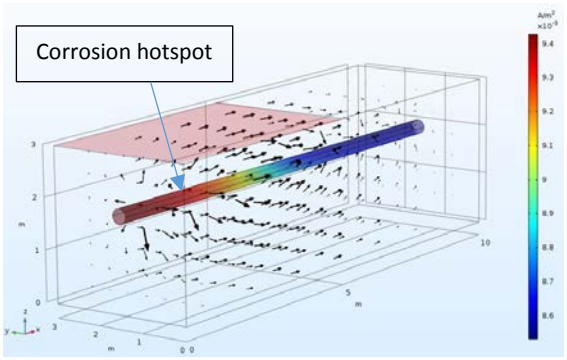

Figure 2: Corrosion current density on the pipe and electrolyte current flowing through soil, showing corrosion hotspot in covered region (denoted by red shading)

The corrosion rate as given by the iron oxidation current density and the resulting mass loss calculated from Faraday's law were plotted for the covered region. The time dependent corroded mass loss agrees well with the exponential model proposed by Rajani et al [2]. According to Rajani et al., the mass lost due to corrosion or the pit depth P could be expressed as an exponential function as shown below with controlling parameters a,b,c and time t.

$$P = at + b(1 - e^{-ct}) \quad (21)$$

The corrosion rate is obtained by differentiating this expression with respect to time to get,

$$\frac{dP}{dt} = a + bce^{-ct} \quad (22)$$

This indicates that the maximum corrosion rate, equal to $a + bc$ occurs immediately after exposure, at $t = 0$ and gradually decreases with time. The minimum corrosion rate equal to a is obtained when $t \to \infty$. In practical terms this could be interpreted as a short term and long term corrosion rates given by the gradients of the above exponential curve initially and at the quasi-steady state after a significant period of time. These trends are seen in the mass loss and corrosion current densities obtained by the simulation. Changing the units of time into years and fitting the model data to the exponential curve results in a very good fit (figure 3) and gives the following values for constants- a=0.1216, b=5.447, c=0.6934 (R-square: 0.9987, RMSE: 0.05556). Overall, the evolution from the high initial short term corrosion rates to the much lower long term corrosion rates over time is captured well with this model and also agrees to the average

time scales and mass losses in experimental data presented in the NBS corrosion study conducted by Romanoff [1].

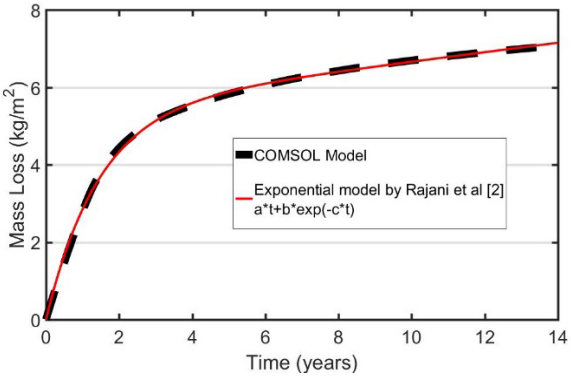

Figure 3: corrosion data from model fitted to the exponential model by Rajani et al [2]

The short term corrosion rates (calculated at t =100 days) at different degrees of saturation S_r show that the corrosion rate increases gradually with increasing soil saturation up to an optimum value around S_r = 0.7 after which it starts to decrease. This relationship of an optimum moisture content has been obtained experimentally by several researchers [23], [25], [26]. The increase of corrosion rate initially is attributed to the increasing soil conductivity with moisture and the drop is due to the diffusion limitation of oxygen at higher saturations due to filling up of pore spaces in the soil. Both of these mechanisms are accounted for in this model thus confirming the experimental observations.

6 Conclusions

Finite element modelling using COMSOL Multiphysics® was revealed to be a useful tool to represent the underground corrosion as influenced by differential aeration. The following conclusions were drawn from the present study.

1. The combined effects of differential aeration and passivation due to corrosion products result in the formation of macro corrosion cells and lead to the corrosion of the pipe sections in regions with poor access to oxygen.
2. The time dependent mass loss and corrosion rates show excellent agreement with empirical relationships in literature.
3. The existence of an optimum moisture content for underground corrosion as experimentally shown by researchers has been confirmed with this model by incorporation of the relevant mechanisms giving rise to it.

If combined with experimental and field evidence, finite element models could provide valuable insights regarding underground corrosion which could be easily incorporated into pipe condition assessment efforts.

7 References

[1] M. Romanoff, *Underground Corrosion*. Washington DC: United States Department of Commerce, 1957.

[2] B. Rajani, J. Makar, S. McDonald, C. Zhan, S. Kuraoka, C. K. Jen, and M. Veins, *Investigation of Grey Cast Iron Water Mains to Develop a Methodology for Estimating Service Life*. AWWA Research Foundation and American Water Works Association, 2000.

[3] G. Doyle, M. V Seica, and M. W. F. Grabinsky, "The role of soil in the external corrosion of cast iron water mains in Toronto, Canada," *Can. Geotech. J.*, vol. 40, no. 2, pp. 225–236, 2003.

[4] N. D. Tomashov, "Underground corrosion of metals," in *Theory of Corrosion and Protection of Metals*, 2nd ed., Macmillan, 1966, 1966, pp. 399–421.

[5] E. Levlin, "Aeration Cell Corrosion of Carbon Steel in Soil: In situ Monitoring Cell Current and Potential," *Corros. Sci.*, vol. 38, no. 12, pp. 2083–2090, Dec. 1996.

[6] R. N. Deo, R. M. Azoor, and J. K. Kodikara, "Proof of concept using numerical simulations for pipe corrosion inferences using ground penetrating radar," in *Advanced Ground Penetrating Radar (IWAGPR), 2017 9th International Workshop on*, 2017, pp. 1–5.

[7] R. B. Petersen and R. E. Melchers, "Long-Term Corrosion of Cast Iron Cement Lined Pipes," *Corros. Prev.*, vol. 23, pp. 1–12, 2012.

[8] L. S. Selwyn, W. R. Mckinnon, and V. Argyropoulos, "Maney Publishing Models for Chloride Ion Diffusion in Archaeological Iron," vol. 46, no. 2, pp. 109–120, 2001.

[9] N. D. Tomashov, *Passivity and Protection of Metals Against Corrosion*. Springer US, 1967.

[10] S. Rathnayaka, B. Shannon, C. Zhang, and J. K. Kodikara, "Introduction of leak-before-break (LBB) concept for cast iron water pipes on the basis of laboratory experiments," 2014.

[11] P. Rajeev, J. Kodikara, D. Robert, P. Zeman, and B. Rajani, "Factors Contributing To Large Diameter Water Pipe Failure As Evident From Failure.," no. September, pp. 9–14, 2013.

[12] S. C. Kranc and A. A. Sagues, "Computation of reinforcing steel corrosion distribution in concrete marine bridge substructures," *Corrosion*, vol. 50, no. 1, pp. 50–61, 1994.

[13] W. J. Schwerdtfeger, "Soil Resistivity as Related to Underground Corrosion and Cathodic Protection.," *J. Res. Natl. Bur. Stand. (1934).*, vol. 69, no. I, 1965.

[14] S. F. Mughabghab and T. M. Sullivan, "Evaluation of the Pitting Corrosion of Carbon Steels and Other Ferrous Metals in Soil Systems,"

vol. 9, no. X, pp. 239–251, 1989.
[15] R. G. Wakelin and R. A. Gummow, “A Summary of the Findings of Recent Watermain Corrosion Studies in Ontario,” *NRC Publ. Arch.*, 1993.
[16] R. N. Deo, N. Birbilis, and J. P. Cull, “Measurement of corrosion in soil using the galvanostatic pulse technique,” *Corros. Sci.*, vol. 80, pp. 339–349, 2014.
[17] R. N. Deo and J. P. Cull, “Spectral induced polarization techniques in soil corrosivity assessments,” *Geotech. Test. J.*, vol. 38, no. 6, pp. 965–977, 2015.
[18] Y. Mualem and S. P. Friedman, “Theoretical Prediction of Electrical Conductivity in Saturated and Unsaturated Soil,” *Water Resour. Res.*, vol. 27, no. 10, pp. 2771–2777, 1991.
[19] J. D. Rhoades, P. A. C. Raats, and R. J. Prather, “Effects of Liquid-phase Electrical Conductivity, Water Content, and Surface Conductivity on Bulk Soil Electrical Conductivity,” *Soil Sci. Soc. Am. J.*, vol. 40, no. 5, p. 651, 1976.
[20] R. J. Millington and J. P. Quirk, “Permeability of porous solids,” *Trans. Faraday Soc.*, vol. 57, no. 0, pp. 1200–1207, 1961.
[21] M. Aachib, M. Mbonimpa, and M. Aubertin, “Measurement and Predictions of the Oxygen Diffusion Coefficient in Unsaturated Media, With Applications to Soil Covers,” *Water. Air. Soil Pollut.*, vol. 156, pp. 163–193, 2004.
[22] D. N. Dang, L. Lanarde, M. Jeannin, R. Sabot, and P. Refait, “Influence of soil moisture on the residual corrosion rates of buried carbon steel structures under cathodic protection,” *Electrochim. Acta*, vol. 176, pp. 1410–1419, 2015.
[23] R. Akkouche, C. Rémazeilles, M. Jeannin, M. Barbalat, R. Sabot, and P. Refait, “Influence of soil moisture on the corrosion processes of carbon steel in artificial soil : Active area and differential aeration cells,” *Electrochim. Acta*, vol. 213, pp. 698–708, 2016.
[24] Y.-C. Chang, R. Woollam, and M. E. Orazem, “Mathematical Models for Under-Deposit Corrosion: I. Aerated Media,” *J. Electrochem. Soc.*, vol. 161, no. 6, pp. C321–C329, 2014.
[25] S. K. Gupta and B. K. Gupta, “The critical soil moisture content in the underground corrosion of mild steel,” *Corros. Sci.*, vol. 19, no. 3, pp. 171–178, 1979.
[26] C. P. Gardiner and R. E. Melchers, “Corrosion of mild steel by coal and iron ore,” vol. 44, pp. 2665–2673, 2002.